Journal of Applied Pharmaceutical Research
Volume 12 Issue 4, Year of Publication 2024, Page 83 – 98
DOI: https://doi.org/10.69857/joapr.v12i4.610

Check for updates

Research Article

JOURNAL OF APPLIED PHARMACEUTICAL RESEARCH | ***JOAPR***
www.japtronline.com ***ISSN: 2348 – 0335***

DESIGN, DEVELOPMENT, AND OPTIMIZATION OF SUMATRIPTAN LOADED ETHOSOMAL INTRA-NASAL NANOGEL FOR BRAIN TARGETING

Nagadivya Nerella, Bakshi Vasudha*

Article Information
Received: 24th April 2024
Revised: 21st June 2024
Accepted: 12th July 2024
Published: 31st August 2024

Keywords
Film hydration, vesicle size, zeta potential, intranasal delivery, ex vivo permeation, central composite design

ABSTRACT
Background: Sumatriptan is one of the most essential drugs for treating migraine. However, dosage-related side effects are still a worry despite its 14 % oral bioavailability and recurrence of migraine-associated diseases. **Methodology:** The fundamental focus of the study is to develop the sumatriptan intra-nasal nano-ethsomal gel by film hydration technique with the aid of QbD principles that govern the varied compositions and blends of polymers like HPMC K100M and Phospolipon 90G to develop a sustained release dosage form. **Results and discussion:** The preliminary FT-IR and DSC studies revealed no interactions between the drug and their physical mixtures. The present study considered three observable responses: vesicle size, zeta potential, and percent drug release after 24 h, taken into consideration during the optimization of the ethosomal formulations utilizing 3^2 central composite designs (CCD). The vesicle size (122.23 nm), zeta potential (-40.2 mV), and drug release percentage (92.61 %) for all formulations were seen in the F12 batch after 24h. The p-XRD and SEM studies indicated that the nano-ethosomal gel was stable. The stability studies indicated the preparation of a more stable formulation for the parameters under the study protocol. **Conclusion:** Using a novel intra-nasal brain targeting approach by adapting the film hydration technique, the current issues might be addressed, and the drug's duration of residence at the absorption site uptake substantially increase. To efficiently modify the drug's residence through the intra-nasal route, this work focuses on developing a nano-ethosomal gel loaded with sumatriptan.

INTRODUCTION

Sumatriptan is a potent and selective serotonin (5-HT1B/1D) receptor, agonist also known as 1-[3-[2-(dimethylamino) ethyl]-1H-indol-5-yl]-N-methylmethanesulfonamide. It is a second-generation triptan and is used in the acute treatment of migraine attacks with or without aura and cluster headaches [1]. Migraine is often associated with nausea, vomiting, and gastric stasis, which makes the oral route unsuitable. It is also reported that the oral bioavailability of SUT is only 14% due to the hepatic first-pass effect, and the half-life is 2-3 h, so it requires frequent administration [2]. As an episodic condition of a migraine, later on, it may become chronic, so there is a need to develop a

*School of Pharmacy, Anurag University, Venkatapur, Ghatkesar Rd, Hyderabad, Telangana 500088, India

For Correspondence: **deanpharmacy@anurag.edu.in**

sustained release dosage form as an alternate route of administration [3-5]. Sumatriptan (SUT) narrows brain blood vessels by activating serotonin receptors, naturally occurring brain chemicals [5, 6]. Although several good migraine treatments have been created utilizing nasal delivery, most have not been proven commercially viable [7-9]. Some triptans can be administered nasally, demonstrating effective and fast action for relieving migraine attacks. (SUT) has low penetration to the central nervous system (CNS). SUT exhibits low oral bioavailability, ranging from 14% to 20%, with a shorter half-life of 1.7 h, coupled with its poor oral bioavailability, making it a potential target for nanotechnology delivery to improve its bioavailability. Migraines can vary significantly from person to person regarding triggers, symptoms, and treatment response. Some patients may not respond to first-line treatments, such as over-the-counter medications or prescribed triptans [8]. Migraines are often chronic conditions requiring ongoing management, which can be burdensome for patients regarding time, effort, and emotional strain [6]. Since the main target is the brain, the intranasal route can be chosen to represent the optimal delivery to the brain; additionally, this route will reduce its systemic side effects. To overcome these restrictions, a nano-formulation that targets the brain and delivers a prolonged release of medication is required. Such approaches that may be used to circumvent the blood-brain barrier and operate as a medication carrier is the nano-ethosomal drug delivery system, is facilitated via the olfactory lobes route [8, 9]. Ethosomes are special liposomes manufactured utilizing a highly concentrated alcohol solution [10]. This study progresses, using the screening design of Taguchi followed by optimization by 3^2 central composite design (CCD) to construct and improve SUT-loaded ethosomal gel. Using HPMC K100M as a mucoadhesive agent, poloxamer 407 as a gelling agent, and Phospholipon 90G as a phospholipid, the prepared optimized ethosomes were assessed and subsequently integrated into thermo-sensitive gel form.

MATERIALS AND METHODS

Materials

Sumatriptan (SUT) was obtained as a free sample from Sun Pharma Ltd., Mumbai, India. Phospholipids, i.e., Phospholipon (90G) (10, 20, 40 mg/ml), and HPMC K100M (2% w/v), were purchased from Sigma Aldrich. Ethanol, methanol, propylene glycol, acetonitrile, and other solvents were purchased from Merck Ltd., India. All other chemicals and reagents were obtained from local suppliers and of analytical grade.

Methods

Pre-formulation studies

Solubility studies

Acetone, ethanol, DMSO, distilled water, phosphate buffers 6.8 and 7.4, 0.1N HCl, methanol, acetonitrile, DMF, PEG 200, and 400 were all used to test the drug's solubility. Each solvent was mixed with a suitable amount of the SUT, and the mixture was shaken for 72 hours in a mechanical shaker (Model: Reciprocating (Horizontal) 50111001 Rivotek, Riviera Glass Pvt. Ltd.) in a water bath at a temperature maintained at 37±0.5°C. The drug's complete solubilization in the vials was regularly checked. To get rid of any drugs that were intractable or immiscible, all mixes were permitted to be put into centrifuge tubes [11, 12].

UV estimation of SUT (SUT) in acetonitrile

100 mg of SUT was carefully weighed and fully dissolved in 10 mL acetonitrile, and the volume was then increased to the needed mark of 100 mL to provide a stock solution of 1000 µg/ml (ppm). Then, employing acetonitrile, 10 mL of the standard working solution was diluted to 100 mL to obtain a 100 µg/ml (ppm) concentrated solution (Model no. UV-visible spectrophotometer UV-1800 Labindia Ltd., Mumbai, India). These solutions were carefully scanned at 200-400 nm wavelengths. The UV corresponding scan spectrum curve was recorded down the corresponding wavelength, having the maximum absorbance marked for additional dilutions of 2, 4, 8, 10, 12, 14, and 16 µg/mL concentrated solutions. The maximum wavelength of λ_{max} was found to be 228 nm. Serial dilutions were done, and the calibration curve was constructed from 2 to 16 µg/mL with an R^2 value of 0.9778 at λ_{max} 228 nm [13].

UFLC-based estimation of SUT

A Shimadzu liquid chromatographic system with a photodiode array (PDA) detector and an ODS C18 (50 x 3mm; 5 µm) chromatographic column was used to refine the technique. The final optimized trail was obtained using acetonitrile and water (70:30%v/v) as the mobile phase, with a flow rate maintained at 0.5mL/min and a run length of 8 minutes. The injection volume was retained at 20µL with a column oven temperature of 40°C. A PDA detector with a maximum wavelength of 268 nm was applied for chromatographic detection. Ultimately, this novel method is beneficial for the drug SUT [14], with a retention time (Rt) of 4.643 minutes and no peak interference [15].

FT-IR

FT-IR spectrometry (Shimadzu Analytical Pvt. Ltd., India, Model No. Shimadzu IR affinity-1) showed that the drug sumatriptan (SUT) has physical interactions. Potassium bromide was used to create the FT-IR spectra of various physical mixtures of drugs with Phospholipon 90G, HPMC K100M, and the optimized F12 formulation. Transmittance from 4000 to 400 cm-1 was computed to assess the drug-excipient interaction. Peak matching was used to determine if there was any interaction between the pure drug and the other excipients [12].

DSC

To investigate the drug's compatibility with the phospholipid, (Model No. DSC (Differential Scanning Calorimetry) (SHIMADZU DSC-60). Ltd) was used. In aluminum pans, dried nitrogen was used as the effluent gas to warm each specimen (10 mg). The physical combinations of SUT with Phospholipon 90G and HPMC K100M and the optimized F12 formulation were ascertained using DSC thermogram analysis [13].

Identification of quality target product profile (QTPP) and critical quality attributes (CQAs)

A quality-based design (QbD) driven approach was used to develop the formulation. A quality target product profile (QTPP) was first established to formulate the dosage with enhanced performance and therapeutic advantages. Garg et al., to achieve an optimal formulation of nanosized ethosome-based hydrogel formulations of methoxsalen for enhanced topical delivery against vitiligo, the mass of phospholipid and ethanol were considered CMAs, and five responses such as vesicle size, percentage of drug entrapment (PDE), percentage of drug leakage (PDL), permeation flux (J), and skin deposition (SD) were considered CQAs. To achieve an efficient formula, the authors suggested an amount of 2–2.5 for PDL and 5.5–6.5 for J in the CQAs section. As shown in **Table 1**, primary consideration was given to dosage type (sustained), dosage form (intra-nasal gel), and drug release. Essential CQAs were identified as quality characteristics of flexible vesicles, including formulation and physical attributes, to fulfill the requirements of defined QTPP. The most important quality criteria that were found to be responsible for the product's performance were the cumulative drug release at 24 h, vesicle size, and the zeta potential [14].

Formulation of sumatriptan loaded nano ethosomal gel

Using varying quantities of phospholipid (Phospholipon 90G) (20, 30, 40 mg/ml), ethanol (10, 15, and 20 %w/v) as a harvesting solvent, propylene glycol (10% v/v), drug (20 mg), and water (qs 100 % w/w), drug-loaded ethosomal gel was made using the traditional thin film hydration process. Phospholipid was dissolved in a 250 ml round-bottom flask containing a 2:1 v/v ratio of chloroform to methanol. The vacuum was initiated after 30 seconds to extract the solvent entirely. The mixture above was kept constant by heating above the lipid transition temperature (55±2 °C) at 60 rpm until complete evaporation, provided the condenser was refrigerated for effective removal of the organic solvent. After that, the film was hydrated for 30 minutes at 55 ± 2 °C, above the lipid transition temperature, using medication and propylene glycol mixed in ethanolic solution. The lipid was fully swelled to produce vesicular dispersion and then maintained at room temperature for two hours. After that, the obtained dispersion was exposed to three cycles of 15 minutes each (15 s on/off cycle) of probe sonication (Rivotek Ultrasonic Sonicator, Mumbai, India) for 45 minutes. After that, the formulation was refrigerated for further characterization [15, 16].

Table 1: Quality target product profile (QTPPs) and critical quality attributes (CQAs) for developing sumatriptan loaded intra-nasal ethosomal gel

QTTPs	Target	CQAs	Predetermined target	Justification
Dosage type	Sustained release dosage forms	Cumulative drug release at 24h (%)	≥ 80%-95%	Sustained drug release is the study's objective and is important for better drug absorption.
Dosage form	Intra-nasal Ethosomal gel	Vesicle size (nm)	100-200 nm	Highly critical factor as its role in the permeation and retention of bio-actives in the intra-nasal route.
Dosage Stability	Stable nano ethosomes	Zeta potential	±20-40 mV	Highly critical factor as its role in ensuring the stability of the formulation.

Table 2: Factor analysis of materials and process variables using FMEA (Failure Mode and Effects Analysis) tool during the preparation of sumatriptan loaded intra-nasal ethosomal gel

Process parameters	Risk priority number (RPN)	Severity (S)	Occurrence (O)	Detectability (D)
Concentration of phospholipid (Phospholipon 90G) (mg/ml)	294	7	6	7
Temperature	32	4	2	4
Volume of aqueous phase (ml)	36	6	3	2
Concentration of ethanol (% v/v)	392	7	8	7
Stirring speed(rpm)	140	4	5	7
Stirring Time (min)	150	6	5	5
Stirring type	120	5	4	6
Sonication speed per time	168	6	4	7

Table 3: Design matrix for the influential factors screening as per Taguchi Design, along with the experimental results of selected CQAs

Run	Factor 1	Factor 2	Factor 3	Factor 4	Factor 5	Factor 6	Factor 7	Response 1	Response 2	Response 3
1	Level 1 of A	Level 2 of B	Level 2 of C	Level 1 of D	Level 1 of E	Level 2 of F	Level 2 of G	66.85	259.45	-9.5
2	Level 2 of A	Level 2 of B	Level 1 of C	Level 2 of D	Level 1 of E	Level 1 of F	Level 2 of G	39.23	435.46	-4.1
3	Level 2 of A	Level 1 of B	Level 2 of C	Level 1 of D	Level 2 of E	Level 1 of F	Level 2 of G	47.45	365.36	-5.4
4	Level 1 of A	Level 1 of B	Level 1 of C	Level 2 of D	Level 2 of E	Level 2 of F	Level 2 of G	87.23	202.9	-15.2
5	Level 2 of A	Level 1 of B	Level 2 of C	Level 2 of D	Level 1 of E	Level 2 of F	Level 1 of G	50.36	315.23	-6.5
6	Level 1 of A	Level 1 of B	Level 1 of C	Level 1 of D	Level 1 of E	Level 1 of F	Level 1 of G	79.58	232.56	-12.5
7	Level 2 of A	Level 2 of B	Level 1 of C	Level 1 of D	Level 2 of E	Level 2 of F	Level 1 of G	40.23	385.22	-4.2
8	Level 1 of A	Level 2 of B	Level 2 of C	Level 2 of D	Level 2 of E	Level 1 of F	Level 1 of G	58.34	295.47	-7.5

Response 1: Cumulative drug release at 24h (%); Response 2: Particle size (nm); Response 3: Zeta Potential (mV)

S No.	Factors	Codes	Low level (-1)	High level (+1)
1	Concentration of phospholipid (Phospholipon 90G) (mg/ml)	A	10	20
2	Concentration of ethanol (% v/v)	B	5	15
3	Stirring speed (rpm)	C	1000	2000
4	Stirring time (min)	D	30	60
5	Stirring type	E	Mechanical	Magnetic
6	Sonication speed per time (Hz/Minute)	F	1000/10	2000/20
7	Drying time(min)	G	10	20

Analysis of risk assessment

Risk assessment studies were used to examine several quality aspects related to ethosomes. The Ishikawa fishbone diagram for ethosomes creation was used in the process. The primary goal is to explore the cause-and-effect connection between several process parameters (PPs) and Critical material characteristics (CMAs), as well as the anticipated impact of these on the exosomes CQAs. Failure mode and effect analysis (FMEA) was used to identify the critical risk variables that significantly impacted the chosen CQAs [17, 18]. The risk priority number

(RPN) was determined by assigning rank order scores (Ranging from 1 to 10), as depicted in **Table 2,** to the material and process parameters attributes based on severity (S), occurrence (O), and detectability (D) through an extensive literature survey, prior knowledge, and brainstorming exercises.

Using Taguchi orthogonal array (OA design) for preliminary screening

To determine the most significant element or factors preventing the CQAs, an initial evaluation was carried out using a Taguchi design consisting of seven components and two tiers, as shown in **Table 3**. Eight different formulations for the Taguchi design of the experiment matrix were created and constructed, along with an assessment of the CQAs that were given. An ANOVA was used to determine each aspect's overall importance, as shown in **Table 4**. To assess the crucial components, the p-value was finally actualized [19].

Table 4: Summary of ANOVA for factor screening and its significance as per Taguchi design

Factors	p-values of obtained from screened responses		
	Cumulative drug release at 24h (%)	Vesicle size (nm)	Zeta potential(mV)
Concentration of phospholipid (Phospholipon 90G) (mg/ml)	0.0044*	0.0036*	0.0078*
Concentration of ethanol (% v/v)	0.0122*	0.0005*	0.0125*
Stirring speed (rpm)	0.0236*	> 0.1000	0.0245*
Stirring time (min)	> 0.1000	> 0.1000	0.125
Stirring type	0.226	0.0826	> 0.1000
Sonication speed per time (Hz/Minute)	0.0269*	0.0025*	0.0265*
Drying time(min)	0.069	0.0269*	0.0365*

*Significant values, i.e., less than α value (0.05)

Statistical optimization of ethosomal intranasal gel of SUT by central composite design

To maximize the many essential material properties impacting the response variables or critical quality attributes, a two-factor, three-level Central Composite design was used, as shown in **Table 5**. Three distinct degrees of variation were observed in the concentration of Phospholipon 90G (mg/ml) (X1) and Concentration of Ethanol (% v/v) (X2), which were identified as separate essential material qualities. Three dependent quality attributes were evaluated: vesicle size (Y3), Zeta potential (Y2), and Cumulative drug release at 24h (%) (Y1). Thirteen batches were made, with four center points for each block. Design Expert software (Design Expert 13, Stat-Ease, Minneapolis, MN) was fitted with the acquired data.

Response surface studies were performed to understand the connection between the variables and their interaction, and contour plots and (3D) response surface plots were generated. Second-order polynomial models were created and put into a multiple linear regression model to determine the impact of various CMAs on CQAs. Design validation was carried out using analysis of variance (ANOVA) [20]. Quality attribute constraints were established at goal levels, and potential formulation composition was ascertained using Design Expert software's checkpoint analysis and desirability technique. A numerical optimization process using the desirability function was used to choose the best formulation [21, 22].

Characterization of SUT-loaded ethosomes

Entrapment efficiency

When the deformable vesicles, or ethosomes, were separated from the solution using the centrifugation procedure, the drug entrapment effectiveness of the ethosomes was recorded. The estimated process included extracting 10 milliliters of SUT-loaded ethosomal dispersions and centrifuging them for one hour at -4°C for 50,000 rpm using a cooling centrifuge (Model: Eltec Lab RC 4815). The centrifugation dialysis procedure partially removes the unentrapped free medication [23]. The supernatant liquid was collected and subjected to UV spectrophotometric analysis at a wavelength of 228 nm (UV 1800, Shimadzu, Japan) to determine the presence of the free drug, calculated, as shown in Equation 1.

$$\% \, Entrapment \, efficiency = \frac{Total \, drug \, quantity - Quantity \, of \, free \, drug}{quantity \, of \, total \, drug} \, x \, 100 \quad [Eq. 1]$$

Table 5: Different formulation composition of sumatriptan loaded intra-nasal ethosomal gel of obtained thirteen experimental runs as per central composite design (CCD) along with the obtained CQAs responses

Runs	Sumatriptan (mg)	Factor 1 (X1)	Factor 2 (X2)	Response (Y1)	Response (Y2)	Response (Y3)
1	20	0	0	62.35	-30.4	190.33
2	20	-1	0	27.34	-12.6	320.66
3	20	0	-1	34.69	-19.6	298.61
4	20	-1	1	30.22	-15.4	318.52
5	20	1	0	75.69	-31.4	135.26
6	20	0	0	59.68	-30.9	202.33
7	20	-1	-1	15.92	-6.5	568.3
8	20	0	0	52.66	-27.6	219.6
9	20	0	0	45.01	-25.9	350.3
10	20	0	1	72.65	-32.6	149.67
11	20	1	-1	35.66	-20.3	294.78
12	20	1	1	92.61	-40.2	122.33
13	20	0	0	40.11	-22.3	260.3

	Coded and actual levels		
Independent Variables	**Low (−1)**	**Medium (0)**	**High (+1)**
A: Concentration of Phospholipon 90G (mg/ml)	20	30	40
B: Concentration of ethanol (% v/v)	10	15	20

Vesicle size, polydispersity index (PDI) and zeta potential determination

The Malvern equipment (Model: Malvern ZETASIZER NANO ZS Malvern ZEN3600 RED) was equipped with (PCS) photon correlation spectroscopy to measure the vesicle size. This spectroscopy was assumed to estimate and evaluate the particle size and zeta potential. Typically 10-200 nm nanoparticles can effectively pass through biological barriers, such as the blood-brain barrier (BBB). The length of particles influences their distribution, cellular uptake, and overall therapeutic effectiveness. The polydispersity index was computed, and a size distribution was provided. Zeta potential levels significantly impact the homogeneity within the ethosomal dispersion [24-26].

Scanning electron microscopy (SEM)

The improved formulation's morphologic analysis was carried out using a TEM (JEOL JEM1230, Tokyo, Japan) running at an 80 kV accelerating voltage. A single droplet of dispersion was applied to the surface of a copper grid covered with carbon, which was allowed to stick to the carbon substrate for a minute. Any remaining dispersion was then eliminated using a filter paper tip [27].

Powder X-ray Diffraction (p-XRD)

The diffraction experiments were performed using a powder X-ray diffractometer (Model: Rigaku, Japan, Smart Lab 9 kW). The samples were scanned for powder XRD after exposure to nickel-filtered CuKa radiation (40 kV, 30 mA). The data were plotted as peak height (intensity) vs. time (h) using SUT pure medication and improved ethosomal formulation [28].

In-vitro release studies of SUT-loaded ethosomal gel

The drug release from various SUT-loaded ethosomal gels was investigated using the USP Dissolution Test device (Pharma Test Dissolution Tester, Germany). In this in-vitro drug release investigation, the dialysis bag diffusion technique (Himedia; Dialysis Membrane-60; Average flat width: 25.27 mm, Average diameter: 15.9 mm with 10000 kDa–12000 KDa with 5 mL capacity) was utilized for SUT loaded ethosomal gel, which is equal to 2 mg SUT. Five milliliters of each formulation were put into a dialysis membrane, sealed, and submerged in 150 mL of 0.1N HCl under sink conditions for the first 2 h. After that, it

was submerged for 24 hours in a 7.4 pH phosphate buffer solution. The system was kept at 37°C with 500 rpm continuous magnetic stirring. After that, samples (2 mL) were taken out at pre-arranged intervals (0.5, 1, 2, 3, 4, 5, 6, 7, 8, 24 hours) and replaced with 0.1 N HCl and pH 7.4 phosphate buffer. to sustain sink conditions, UV spectrophotometrically measured at λ_{max} 228 nm with a blank of PBS (pH=7.4). The findings were reported as means (n = 3 ± SD) [29].

Ex vivo skin permeation studies

Research on ex vivo permeation was carried out on the goat nasal cavity, obtained from a local slaughterhouse [30-32]. The goat nasal cavity's mucosa was separated from it. After removing the cartilage and blood, the isolated nasal mucosa was washed and preserved in newly made phosphate-buffered saline (pH 6.4). Six systems of Franz diffusion cells with thermostat capabilities were used for the experiment. Nasal tissues were chosen for the investigation and immersed for one hour in the diffusion medium (Phosphate-buffered saline, or PBS; pH 7.4). While the receptor compartments were filled with phosphate buffer pH 7.4, the donor compartment of Franz diffusion cells was covered with nasal tissues with an operational permeation area of 2 × 2 cm^2. The investigation was conducted with an ideal stirring speed of 34 ± 1°C [31, 32]. Concurrently, 200 µl of SUT-laden ethosomal gel, or 2.5 mg, was put into the donor compartment. Samples (0.5 mL) were removed from the receptor compartment and replaced with new buffer for 24 h at the predetermined intervals of 1, 2, 4, 6, 8, 12, and 24 h. At 268 nm, the samples were examined using a UFLC. Under steady-state circumstances, the effective permeability coefficient (mm/s) across the goat nasal mucosa was computed using Equation 2:

$$Permeability\ coefficient = \left(\frac{dc}{dt}\right) ss\ X \frac{V}{A\ Cd} \ldots . [Eq. 2]$$

Where (dc/dt) ss (µg ml^{-1} s^{-1}) is the change of concentration under steady state; A (cm^2) is the permeation area; V (ml) is the volume of the receiver compartment; and Cd (µg ml^{-1}) is the initial donor concentration.

Stability analysis

Stability experiments were conducted on optimized ethosomal formulation in order to assess the impact of various storage conditions. For the duration of the investigation, the formulations were maintained at room temperature (25 ± 2 °C/60 ± 5% RH) and refrigerated condition (4 ± 2 °C). Physical and chemical stability of the formulation were assessed at intervals of 0, 1, 3, and 6 months. Analysing drug release at 24 hours, vesicle size, and formulation entrapment effectiveness percentage allowed for the study of physical stability [33].

RESULTS AND DISCUSSION

Solubility study analysis

The drug solubility in several solvents is shown in **Figure 1A**. The solubility of SUT is maximum in acetonitrile (5326.5±0.25 µg/ml) and acetone (2695.36±0.69 µg/ml) among all other solvents. The RPN bar graph representation of different factors is shown in **Figure 1B**

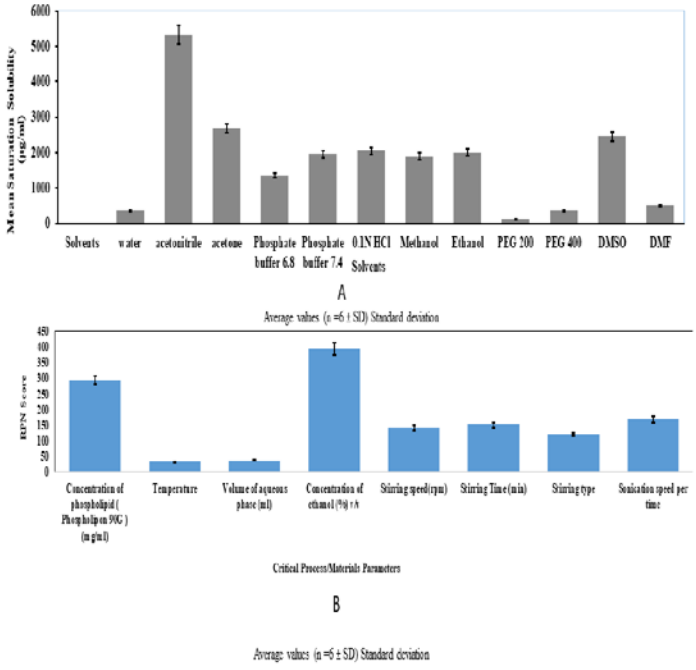

Figure 1: Mean solubility of SUT in different solvents (A), and RPN bar graph representation of different factors (B)

Spectrophotometric estimation of SUT in 0.1N HCl

Following a comprehensive examination of the interference caused by solvents, SUT was determined spectrophotometrically against Acetonitrile, and a calibration curve was created for SUT at λ_{max} 228 nm. As shown in **Figure 2 (A-C)**, the correlation co-efficient (R^2= 0.9778) and linear correlation in the 2-16 µg/ml of SUT range were calculated.

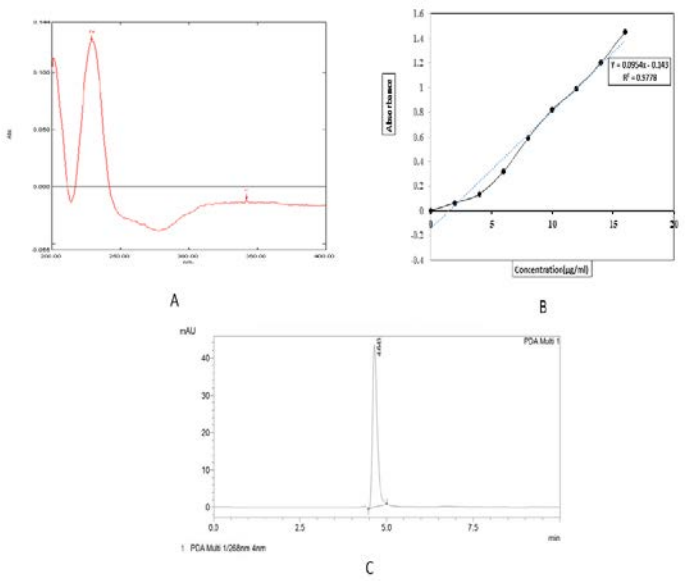

Figure 2: UV spectra of pure drug of sumatriptan in acetonitrile (A), standard curve of sumatriptan at 228nm (B), and UFLC chromatogram of sumatriptan at λ_{max} 268nm (C)

FT-IR Studies

The bands resulting from C=O stretching (1081 cm^{-1}), tertiary amine (3104 cm^{-1}), C–N stretching (1298 cm^{-1}, 1236 cm^{-1}), C–S stretching (634 cm^{-1}), N–H stretching (3376 cm^{-1}) are present in the pure SUT. The similar intensity peaks were also observed in the case of F12 optimized formulation batch along with the additional peaks were observed in physical mixtures which could be due to the presence of polymers and indicated that there was no chemical interaction between sumatriptan and other selected excipients. Therefore, this indicated there is no interactions between the pure drug and the excipients. The FT-IR spectra of pure drug SUT (A) FT-IR spectra of Phospholipon 90G (B) FT-IR spectra of HPMC K100M (C) FT-IR spectra of physical mixture of SUT + Phospholipon 90G + HPMC K100M (D) FT-IR spectrum of F12 formulation (E) are shown in **Figure 3 (A-E)**.

DSC Studies

Figure 4 (A-D) is a representation of DSC thermograms. The DSC spectra of pure drug Sumitriptan showed one endothermic peak at 169.2°C, which is associated with melting point, with corresponding onset and end set temperatures of 164.5°C and 173.9 °C. In addition, the lyophilized formulation (F4) had a pronounced endothermic peak at 152.25 ºC, with start and end set temperatures ranging from 146.71°C to 157.72°C. These results suggested that SUT and the other ingredients in the formulation doesn't exhibited interactions.

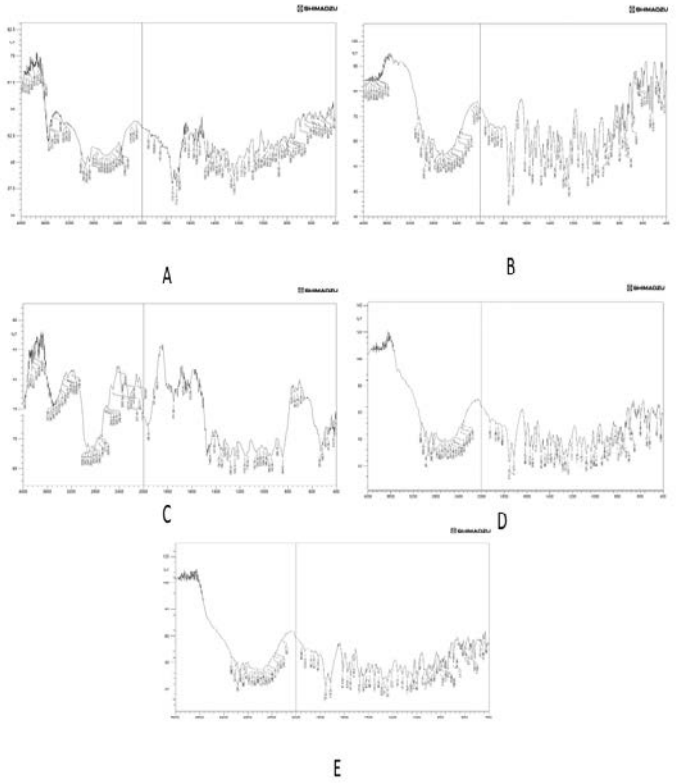

Figure 3: FT-IR spectra of pure drug SUT (A), FT-IR spectra of Phospholipon 90G (B), FT-IR spectra of HPMC K100 (C), FT-IR spectra of physical mixture of SUT + Phospholipon 90G + HPMC K100M (D), and FT-IR spectrum of F12 formulation (E)

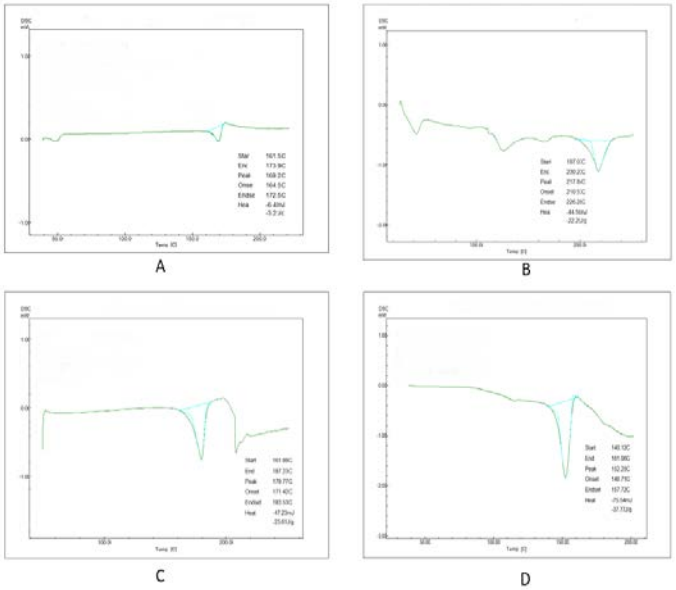

Figure 4: DSC plot of pure drug SUT (A), DSC plot of Phospholipon 90G (B), DSC plot of SUT+ Phospholipon 90G (C), and DSC plot of F12 formulation (D)

Utilizing central composite design and response surface methodology for statistical optimization

The ANOVA and lack of fit were also statistically tested on the model. A substantial p-value was found in the model terms (0.05), and the model was best suited**.** The outlines of the central composite model were determined by fitting it into an appropriate mathematical model, particularly a quadratic model, demonstrating interaction effects among the variables. The direct effect of selected independent factors, such as Concentration of Phospholipon 90G (mg/ml) (A) and concentration of ethanol (%v/v) (B), with additional impact of these individual variables on observed responses cumulative drug release at 24 h (%), and zeta potential (mv) and vesicle size (nm). Moreover, entrapment and drug release were significantly impacted by the Phospholipon 90G content. According to published research, there is a positive correlation between the concentration of Phospholipon 90G and the vesicle size along with drug release. The concentration of ethanol acts as a permeation enhancer within the range of (3 %w/v) that has a significant influence on the drug release. Phospholipon 90G (within the range of 5 %) also contributes to the stability aspect of the ethosomes, because they influence the particle size and entrapment efficiency of the formulation. Drugs that are lipophilic have a tendency to dissolve more readily in lipid, which increases the effectiveness of drug release [34]. Since SUT is lipophilic by nature, it dissolves easily in Phospholipon 90G, indicating that Phospholipon 90G concentration is the primary factor influencing the entrapment efficiency of the formulation [35]. The optimal formulation, Formulation 12, demonstrated the maximum drug release with the desired vesicle size as shown in the 2D and 3D plots of **Figure (5) (A-F)**. Meanwhile, the ethanol concentration simultaneously plays a synergistic role in solubilizing lipophilic drugs, subsequently enhancing entrapment efficiency and drug release of the ethosomal vesicles [36]. The mathematical model elucidates the quadratic polynomial equations 3 to 5 for individual responses using equations 3 to 5.

$$Cumulative\ Drug\ Release\ 24h\ (\%) = +41.63 + 19.06 * A + 14.41 * B + 10 = 12.15 * AB \dots\dots\dots\dots\dots [Eq.3]$$

$$Zeta\ potential(mV) = +42.33 + 22.63 * A + 25.29 * B [Eq.4]$$

$$Vesicle\ size(nm) = +221.61 - 70.87 * A - 55.45 * B - 50.49 * AB \dots\dots\dots\dots\dots [Eq.5]$$

2D and 3D response surfaces' interpretations

Effect of the factor on cumulative drug release 24 h (%)

Figure (5) (A and **B)**. show the contour plot and 3D plot for the CQA cumulative % drug release 24 h. Comparing these formulations, trial run No. 12 seemed to have the greatest percentage of drug release, at 92.61%. Run 7 shows a minimum value of 15.92%, indicating more than 90% drug release in 24 h. Based on the simulations, this reddish zone is predicted to be prevalent at a high level (+1) of Phospolipon 90G conc. and a high level (+1) of ethanol concentration. However, the blue zone with the least amount of drug release was shown to be prevalent at low levels (-1) of Phospolipon 90G conc. and ethanol concentration.

Effect of the factor on zeta potential (mV)

Figure (5) (C and **D)** show the contour plot and 3D plot of the CQA % zeta potential. A comparison of these formulas indicated that trial run No. 12 seemed to have the greatest zeta value at -40.2 mV the bluish zone, which is expected to be prevalent at a high level (+1) of Phospolipon 90G concentration and a high level (+1) of ethanol concentration, represents the highest zeta values, whereas run number seven has the least at -6.5 mV. However, the presence of the light reddish zone was seen at low levels (-1) of Phospolipon 90G concentration and ethanol concentration.

Effect of the factor on vesicle size (nm)

Figure 5 (E and **F)** shows the CQA vesicle size's contour plot and 3D plot. A comparison of these formulations revealed that trial run No. 12 seemed to have the smallest vesicle size, measuring 122.33 nm. Run No. 7 has the largest vesicle size, measuring 568.3 nm. This dark blue zone indicates the least vesicle size and is expected to be prevalent at a high level (+1) of Phospolipon 90G conc. and a high level (+1) of ethanol concentration. However, the largest vesicle size was seen in the light red zone, prevalent at low levels (-1) of Phospolipon 90G concentration and ethanol concentration, respectively.

Analyses overlay plots to establish the design space

The optimized SUT ethosomal gel, shown as an overlay plot in the figure, was created using the central composite design and included 20 mg SUT:40 mg/ml of Phospholipon 90G and 20%v/v of ethanol concentration. **Figure 6** illustrates the region where changing the concentrations of independent factors may maximize the outcomes of dependent variables. The area shown

in the graph offers many passes that provide the optimal factor values to guarantee the viability of each operational restriction at the same time. The inspection of process or formulation restrictions is provided by the overlay plot.

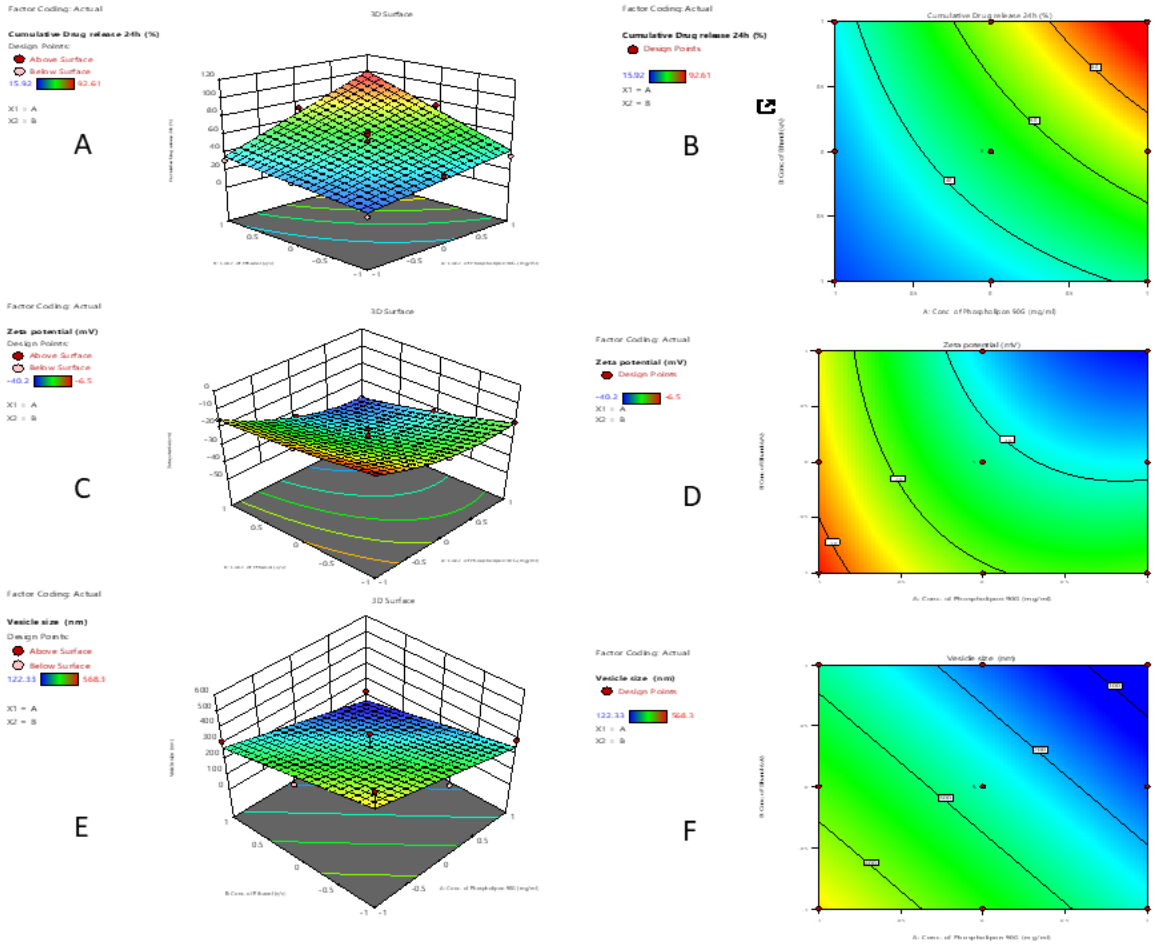

Figure 5: 2D Contour plots and 3D response surface plots of selected independent factors on selected dependant factors such as drug release %, zeta potential, vesicle size [A-F]

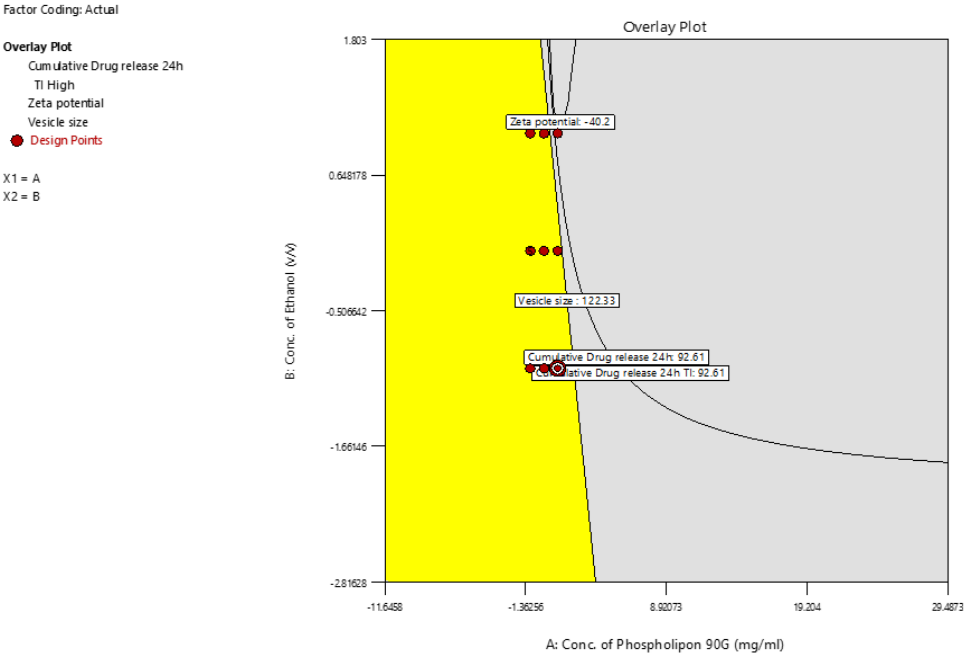

Figure 6: Overlay plot for design space identification

Vesicle size, polydispersity index, and zeta potential

The zeta-sizer instrument analyzed the particle size of all formulations. It was found that some formulations showed a larger particle size. The optimized size range for the F12 formulation was found to be (122.33nm), i.e., for run 12, as shown in Figure 7 (A), which indicates that this vesicular size range will be effective in the drug permeation and absorption through the intranasal route for brain targeting. The developed SUT-loaded ethosomal gel was spherical with uniform particle size distribution. The zeta potential results for the respective formulation were (-40.2mV) for run 12, as shown in Figure 7 (B). A higher absolute zeta potential (positive or negative) indicates greater stability due to stronger electrostatic repulsion between particles, while lower values suggest a tendency for aggregation. **Table 6** shows the obtained values for all 13 formulations on the different characterization parameters, and **Figure 8 (A-D)** represents the bar diagrams for the reported values.

Table 6: Characterization data of thirteen different formulations of sumatriptan-loaded intra-nasal ethosomal gel

Formulation code	Zeta potential (mv)	Polydispersity index	Vesicle size (nm)	Entrapment efficiency (%)
F1	-30.4±0.29	0.369±0.45	190.33±0.65	65.29±0.29
F2	-12.6±0.69	0.325±0.33	320.66±0.26	29.67±0.35
F3	-19.6±0.03	0.258±0.25	298.61±0.36	33.64±0.96
F4	-15.4±0.26	0.297±0.64	318.52±0.59	32.36±0.78
F5	-31.4±0.09	0.345±0.02	135.26±0.05	78.12±0.72
F6	-30.9±0.66	0.224±0.09	202.33±0.02	56.01±0.36
F7	-6.5±0.36	0.129±0.53	568.3±0.04	20.14±0.69
F8	-27.6±0.90	0.397±0.04	219.6±0.08	44.08±0.55
F9	-25.9±0.06	0.373±0.33	350.3±0.06	43.97±0.08
F10	-32.6±0.03	0.459±0.64	149.67±0.54	69.45±0.06
F11	-20.3±0.09	0.449±0.96	294.78±0.66	45.98±0.32
F12	-40.2±0.26	0.423±0.33	122.33±0.64	75.69±0.29
F13	-22.3±0.22	0.29±0.02	260.3±0.69	33.69±0.07

Average values (n =6 ± SD) Standard deviation

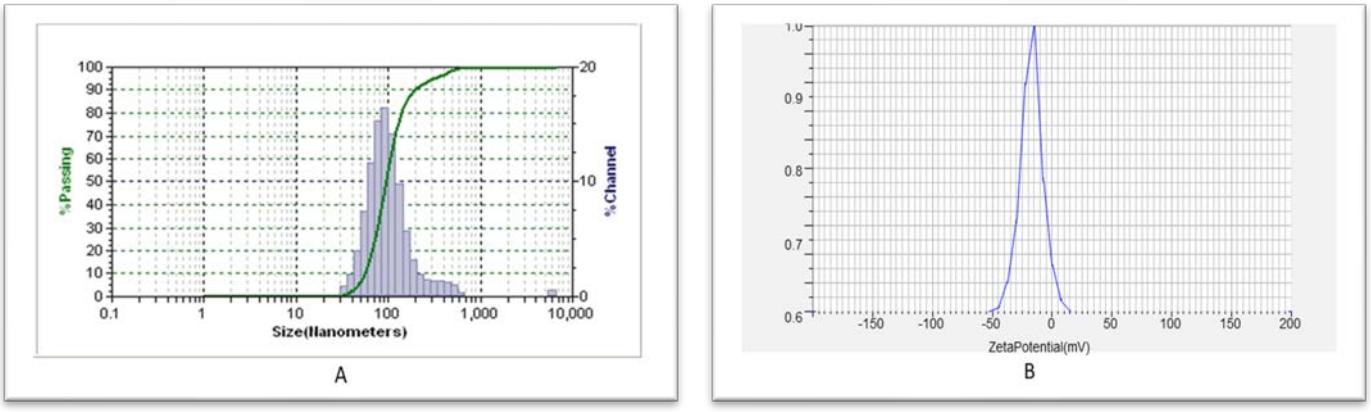

Figure 7: Particle size distribution (A) and zeta potential curves of optimized formulation F12 batch (B)

Scanning electron microscopy (SEM)

Morphological analysis indicates that SEM was used to investigate spherical multilamellar vesicles better. Drug-loaded vesicles with a smooth and spherical form are confirmed by SEM micrograph **Figure 9**. The creation of distorted spherical ethosomes may be caused by the hydrophobic effect, which forms vesicles when aqueous (ethanol and water) and non-polar substances (lipids) are maintained in touch with one another by external pressures (stirring).

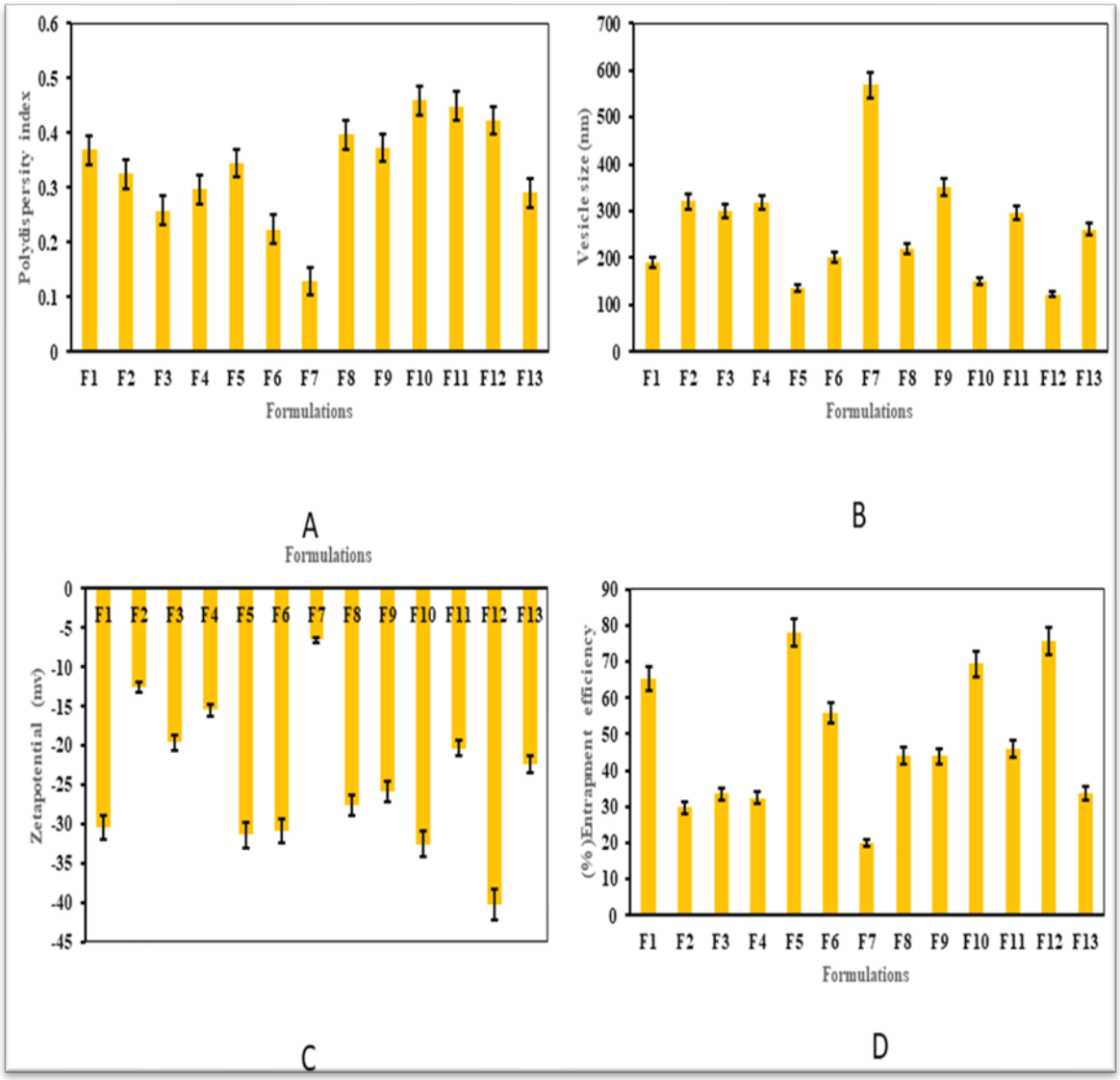

Figure 8: Bar graph representation of characterization parameters such (A) Polydispersity index (B) Vesicle size (nm) (C) Zeta potential (mV) (D) % Entrapment efficiency

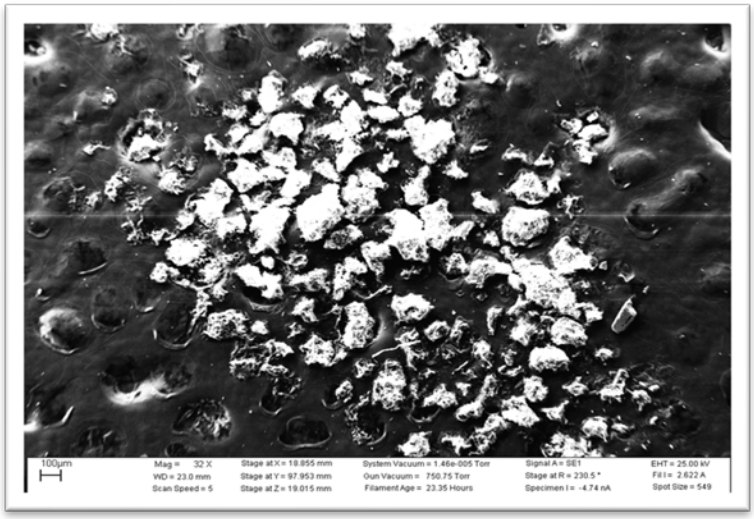

Figure 9: SEM image of optimized batch (F12)

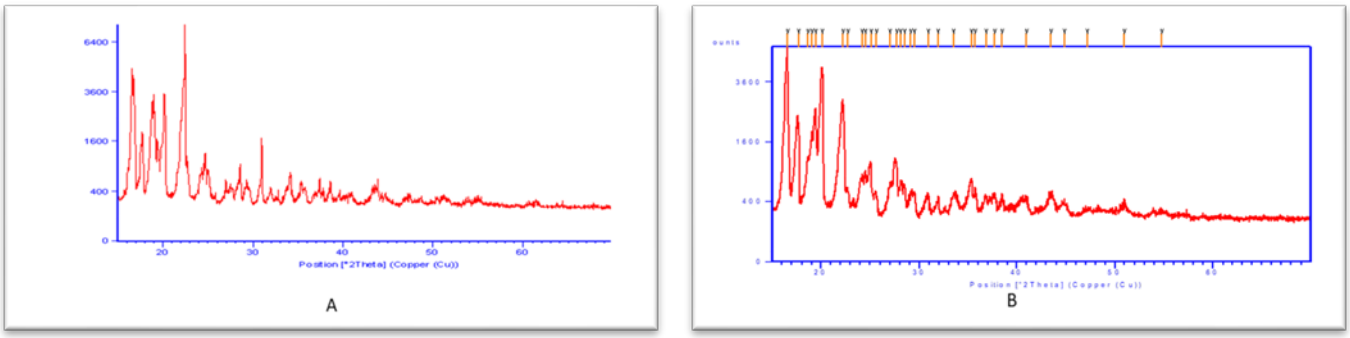

Figure 10: P-XRD curves of (A) pure drug of SUT (B) drug-loaded formulation of SUT (F12)

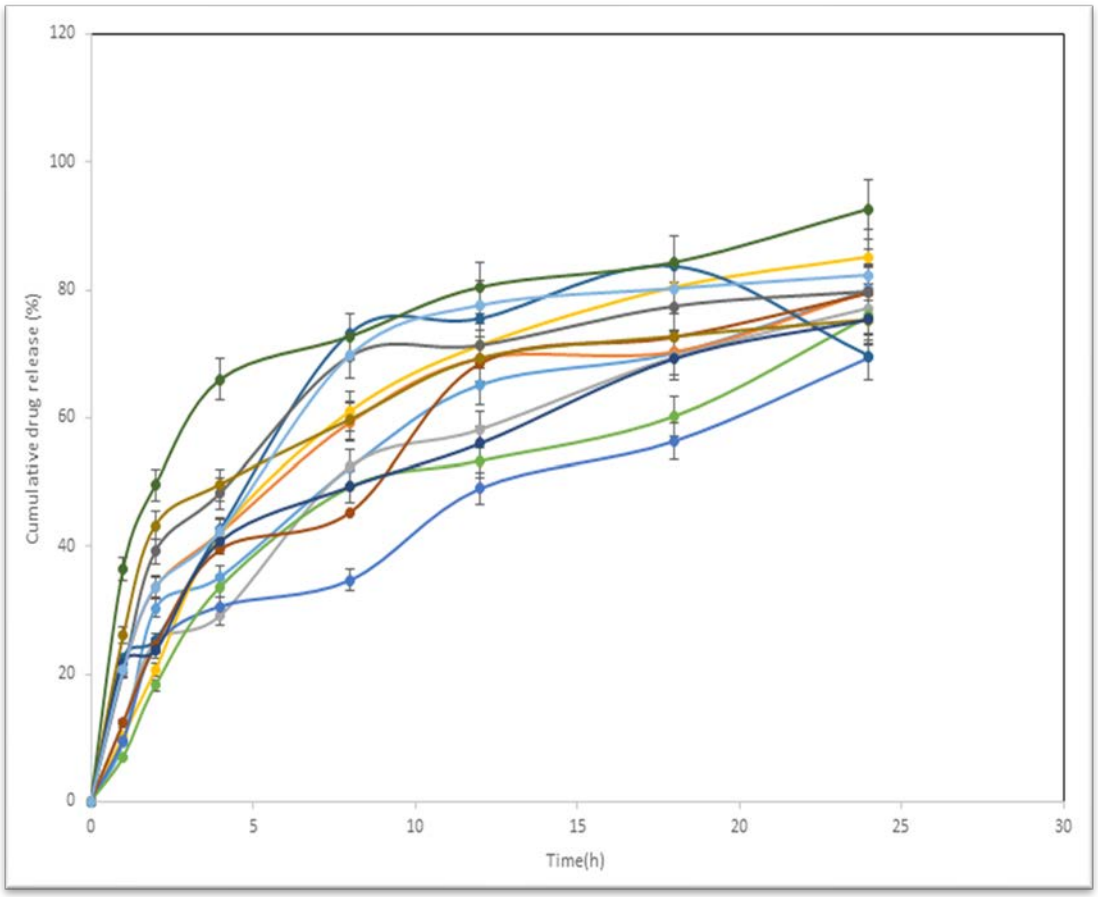

Figure 11: *In-vitro* % drug release of 13 formulated batches of SUT-loaded ethosomal gel. Average values (n =6 ± SD) standard deviation

Powder X-ray Diffraction (p-XRD)

The XRD patterns of optimized SUT-loaded ethosomal gel and that of the pure drug are shown in Figures **10A** and **B,** respectively. Pure-drug SUT showed sharp peaks at the diffraction angles such as 6.9°, 8.3°, 9.9°,19.6° 20.3°, 21.3°, 25.2°, and 26.4°, indicating a typical crystalline pattern. Optimized SUT-loaded ethosomal gel showed a gradual reduction, i.e., the minimal peak intensity at those angles, indicating an amorphous form.

In-vitro release studies of drug-loaded ethosomal gel

Figure 11 suggests a similar drug release profile from gel formulation consisting of HPMC K100M and poloxamer 407. However, drug release after 12 h was more due to the varied ethanol concentration that acted as a permeation enhancer. Optimized ethosomal (SUT) shows a significant in vitro drug release of 96.21% in 24 h compared with the pure drug solution. The Phopholipon 90G concentration at a high level (+1) contributed significantly to the release behavior of the ethosomal

formulation. The 'n' values for a solution and gel formulation were 0.689 and 0.675, respectively, more than 0.5, indicating that the formulated ethosomal gel exhibits the non-Fickian release behavior for the F12 optimized formulation. The release mechanism by curve fitting analysis and the response parameters for SUT loaded ethosomal gel formulation.

Ex vivo skin permeation studies

Figure 12 shows the permeability coefficient of SUT-loaded ethosomal gel formulation across the nasal mucosa with respect to the exposed time of contact with mucosal tissues. Permeation studies on different formulations clearly indicate the permeability of the drug-loaded gel through the nasal mucosa. Ex vivo permeability studies (n=6) demonstrate the identical release profile as in vitro studies where the mucoadhesive agents were the rate-determining.

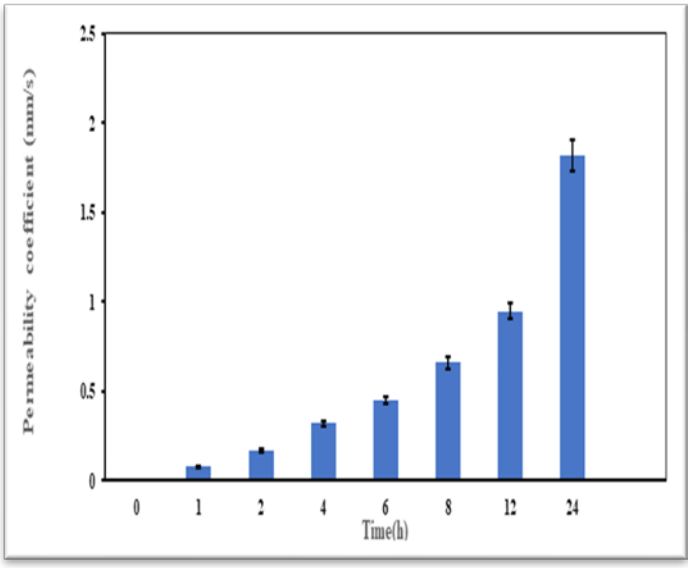

Figure 12: Ex-vivo permeation data of F12 formulation batch. Average values (n =6 ± SD) standard deviation

Stability studies

The P-value is more than 0.05, the value for all the CQAs, indicating there is no significant change. Hence, it can be concluded that the optimized ethosomal gel of SUT was found to satisfy the stability criteria, as there was no substantial change in the CQAs during the study period.

CONCLUSION

In this study, the ethosomal gel of SUT with better dermatological qualities was effectively generated using QbD and DoE principles. The study confirmed that the application of DoE helped identify and optimize the critical processes and material parameters to achieve the desired end product quality criteria. The use of ethosomal intra-nasal gel can aid in the development of patient-compliant and stable vesicles for improved therapeutic benefits, as high concentrations of ethanol and Phospholipon 90G have been identified as the primary critical material attributes that influence vesicle size, entrapment efficiency, and drug release. It was found that with the increase in the Phospholipon 90G concentration of more than 5%, the vesicle size was significantly increased, which may be due to the aggregations of the particles; similarly, the ethanol concentration exhibited a dominant role in the permeability of the drug through the intra-nasal mucosa for brain targeting.

FINANCIAL ASSISTANCE

NIL

CONFLICT OF INTEREST

The authors declare no conflict of interest.

AUTHOR CONTRIBUTION

All authors contributed to the study's conception and design. D. Nerella collected data results and performed analysis, wrote the first draft of the manuscript, and B. Vasudha corrected and revised the manuscript. All authors gave final approval.

REFERENCES

[1] Buse DC, Greisman JD, Baigi K, Lipton RB. Migraine progression: A systematic review. *Headache*, **59**, 306–338 (2018)

[2] Hannon J, Hoyer D. Molecular biology of 5-HT receptors. *Behav Brain Res*, **195**, 198–213 (2008)

[3] Peters GL. Migraine overview and summary of current and emerging treatment options. *Am J Manag Care*, **25**, S23–S34 (2019)

[4] Omar MM, Eleraky NE, El Sisi AM, Ali Hasan O. Development and evaluation of in-situ nasal gel formulations of nanosized transferosomal sumatriptan: Design, optimization, in vitro and in vivo evaluation. *Drug Des Devel Ther*, **13**, 4413-4430 (2019)

[5] Russo AF, Hay DL. CGRP physiology, pharmacology, and therapeutic targets: migraine and beyond. *Physiol Rev*, **103**,1565-1644 (2023)

[6] Girotra P, Singh SK. Multivariate optimization of rizatriptan benzoate-loaded solid lipid nanoparticles for brain targeting and migraine management. *AAPS PharmSciTech*, **18**, 517–528 (2017).

[7] Frimpong-Manson K, Ortiz YT, McMahon LR, Wilkerson JL. Advances in understanding migraine pathophysiology: a bench to bedside review of research insights and therapeutics. *Front Mol Neurosci*, **17**, 1355281 (2024).

[8] Girotra P, Singh SK. A comparative study of orally delivered PBCA and APOE coupled BSA nanoparticles for brain targeting of sumatriptan succinate in therapeutic management of migraine. *Pharm Res*, **33**, 1682–95 (2016)

[9] Hansraj GP, Singh SK, Kumar P. Sumatriptan succinate loaded chitosan solid lipid nanoparticles for enhanced anti-migraine potential. *Int J Biol Macromol*, **81**, 467-76 (2015)

[10] Xu Y, Fourniols T, Labrak Y, Préat V, Beloqui A, des Rieux A. Surface Modification of Lipid-Based Nanoparticles. *ACS Nano*, **16**, 7168-7196 (2022)

[11] Ogundipe OD, Oladimeji FA. Water-in-Oil-in-Water multiple emulsions of ibuprofen for paediatrics using african walnut seed oil. *J App Pharm Res*, **7**, 08-22 (2019)

[12] Pourmand MR, Azar MS. Aghavalijamaat M. Development of validated UV spectrophotometric method for *in vitro* analysis of sumatriptan in pharmaceutical preparations in comparison with HPLC. *Pharm Chem J*, **44,** 585–589 (2011)

[13] Satyanarayana KV, Rao PN. Sensitive Bromatometric Methods for the Determination of Sumatriptan Succinate in Pharmaceutical Formulations. *E J Chemistry*, **8**: 269-275, (2011)

[14] Garg BJ, Garg NK, Beg S, Singh B, Katare OP. Nanosized ethosomes-based hydrogel formulations of methoxsalen for enhanced topical delivery against vitiligo: formulation optimization, in vitro evaluation and preclinical assessment. *J Drug Target*, **24**, 233-246 (2016)

[15] Ghose D, Patra CN, Swain S, Sruti, J. Box-Behnken Design-based development and characterization of polymeric freeze-dried nanoparticles of isradipine for improved oral bioavailability. *Int J App Pharm*, **15**, 60-70 (2023)

[16] Chalmers, JM. Edwards HGM, Hargreaves MD. Infrared and raman spectroscopy in forensic science; Wiley, (2012)

[17] Faroongsarng D. Theoretical aspects of differential scanning calorimetry as a tool for the studies of equilibrium thermodynamics in pharmaceutical solid phase transitions. *AAPS PharmSciTech*, 17, 572-7 (2016).

[18] Swain S, Parhi R, Jena BR, Babu SM. Quality by Design: Concept to applications. *Curr Drug Discov Technol*, **16**, 240-250 (2019)

[19] Rukari T, Pingale PL, Upasani CD. Optimizing novasomes: impact of oleic acid and co-surfactant ratio on posaconazole delivery: In vitro & Ex vivo pharmacokinetic study. *J App Pharm Res*, **12**, 88-98 (2024).

[20] Sallustio V, Farruggia G, Di Cagno MP, et al. Design and characterization of an ethosomal gel encapsulating rosehip extract. *Gels*, **9**, 362 (2023)

[21] Zhang L, Mao S. Application of quality by design in the current drug development. *Asian J Pharm Sci*, **12**, 1-8 (2017)

[22] Mishra V, Thakur S, Patil A, Shukla A. Quality by design (QbD) approaches in current pharmaceutical set-up. *Expert Opin Drug Deliv*, **15**, 737-758 (2018)

[23] Simoes A, Veiga F, Vitorino C. Question-based review for pharmaceutical development: An enhanced quality approach. *Eur J Pharm Biopharm*, **195**,114-174 (2024)

[24] Pramod K, Tahir MA, Charoo NA, Ansari SH, Ali J. Pharmaceutical product development: A quality by design approach. *Int J Pharm Investig*, **6**, 129-38 (2016)

[25] Salem HF, El-Menshawe SF, Khallaf RA, Rabea YK. A novel transdermal nanoethosomal gel of lercanidipine HCl for treatment of hypertension: optimization using box-benkhen design, in vitro and in vivo characterization. *Drug Deliv Transl Res*, **10**, 227-240 (2020)

[26] Qureshi MI, Jamil QA, Usman F, Wani TA, Farooq M, Shah HS, Ahmad H, Khalil R, Sajjad M, Zargar S, Kausar S. Tioconazole-loaded transethosomal gel using box-behnken design for topical applications: In vitro, in vivo, and molecular docking approaches. *Gels*, **9**, 767 (2019)

[27] Iijima M, Hatakeyama T, Hatakeyama H. DSC and TMA studies of polysaccharide physical hydrogels. *Anal Sci*, **37**, 211-219 (2021)

[28] Smirnov I, Kaszkur Z, Hoell A. Development of nanoparticle bulk morphology analysis: a multidomain XRD approach. *Nanoscale*, ***15***, 8633-8642 (2023)

[29] Apolinario AC, Salata GC, de Souza MM, Chorilli M, Lopes LB. Rethinking breast cancer chemoprevention: technological advantages and enhanced performance of a nanoethosomal-based hydrogel for topical administration of fenretinide. *AAPS PharmSciTech*, **23**, 104 (2022)

[30] Praveen A, Aqil M, Imam SS, Ahad A, Moolakkadath T, Ahmad FJ. Lamotrigine encapsulated intra-nasal nanoliposome formulation for epilepsy treatment: Formulation design, characterization and nasal toxicity study. *Colloids Surf B Biointerfaces*, **174**, 553-562 (2019)

[31] Zarrabi A, Alipoor Amro Abadi M, Khorasani S, Mohammadabadi MR, Jamshidi A, Torkaman S, Taghavi E, Mozafari MR, Rasti B. Nanoliposomes and tocosomes as multifunctional nanocarriers for the encapsulation of nutraceutical and dietary molecules. *Molecules*, **25**, 638 (2020)

[32] Bandyopadhyay S, Beg S, Katare OP, Sharma G, Singh B. QbD-Oriented development of self-nanoemulsifying drug delivery systems (SNEDDS) of valsartan with improved biopharmaceutical performance. *Curr Drug Deliv*, **12**, 544-63 (2015)

[33] Gonzalez-Gonzalez O, Ramirez IO, Ramirez BI, O'Connell P, Ballesteros MP, Torrado JJ, Serrano DR. Drug Stability: ICH versus accelerated predictive stability studies. *Pharmaceutics*, **14**, 2324 (2022)

[34] Shelke PV, Rachh PR, Mankar SD, Prasad LG. Optimization and evaluation of transdermal delivery system for nebivolol hydrochloride. *J App Pharm Res*, **12**, 21-37 (2024).

[35] Swain S, Beg S, Singh A, Patro ChN, Rao ME. Advanced techniques for penetration enhancement in transdermal drug delivery system. *Curr Drug Deliv*, **8**, 456-73 (2011)

[36] Phatale V, Vaiphei KK, Jha S, Patil D, Agrawal M, Alexander A. Overcoming skin barriers through advanced transdermal drug delivery approaches. *J Control Release*, **351**, 361-380 (2022)

LIST OF ABBREVIATIONS

CCD: Central Composite design
CQAs: Critical quality attributes
EE: Entrapment efficiency
FT-IR: Fourier-transform infrared spectroscopy
FMEA: failure mode and effect analysis
ICH: The international council for harmonization
QTPP: Quality target product profile
RH: Relative humidity
SD: Standard deviation
SEM: Scanning electron microscopy
SUT: Sumatriptan
TPPs: Target product profiles
UFLC: Ultra-fast liquid chromatography
UV: Ultraviolet Spectroscopy